Analytica Chimica Acta 1133 (2020) 39–47

Contents lists available at ScienceDirect

Analytica Chimica Acta

journal homepage: www.elsevier.com/locate/aca

Engineered glyphosate oxidase coupled to spore-based chemiluminescence system for glyphosate detection

Yuqing Qin [a, b, 1], Gaobing Wu [a, c, 1], Yiming Guo [b], Da Ke [c], Jiakang Yin [a, b], Donglin Wang [b], Xuezhu Fan [a, b], Ziduo Liu [b], Lifang Ruan [a, b, **], Yonggang Hu [a, b, *]

[a] State Key Laboratory of Agricultural Microbiology, Huazhong Agricultural University, Wuhan, 430070, China
[b] College of Life Science and Technology, Huazhong Agricultural University, Wuhan, 430070, China
[c] College of Plant Science and Technology, Huazhong Agricultural University, Wuhan, 430070, China

HIGHLIGHTS

- A glyphosate oxidase preferring glyphosate to produce H_2O_2 was obtained by directed evolution from glycine oxidase.
- The bacillus spores was presented to catalyze luminol-H_2O_2 reaction yielding create excellent chemiluminescence signal.
- Spore-luminol coupling with glyphosate oxidase provided high selectivity and sensitivity detection result for glyphosate.

GRAPHICAL ABSTRACT

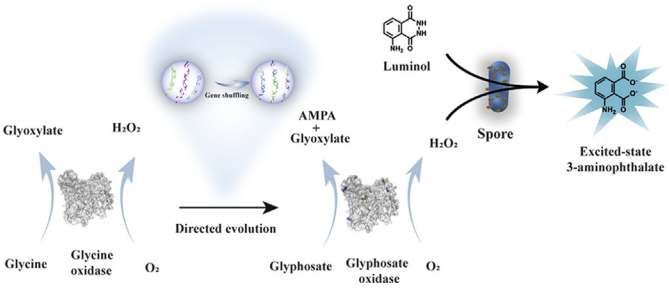

ARTICLE INFO

Article history:
Received 12 March 2020
Received in revised form
29 July 2020
Accepted 30 July 2020
Available online 12 August 2020

Keywords:
Glyphosate oxidase
Directed evolution
Glyphosate
Spore
Chemiluminescence

ABSTRACT

The extensive and intensive utilization of glyphosate (Glyp) caused public concerns on the potential risk of environment and health resulted from the chemical residues. Therefore, the development of a high-selective, low-cost and easy-operation Glyp detection methods is highly desired. Screening highly selective enzymes by directed evolution is important in practical applications. Herein, a glyphosate oxidase (GlypO) preferring substrate Glyp to produce H_2O_2 was obtained via directed evolution from glycine oxidase obtained from *Bacillus cereus* (BceGO). The catalytic efficiency, specificity constant, and affinity enhancement factor of GlypO toward Glyp were increased by 2.85 × 10^3-fold; 2.25 × 10^5-fold; and 9.64 × 10^4-fold, respectively, compared with those of BceGO. The catalytic efficiency toward glycine decreased by 78.60-fold. The spores of *Bacillus subtilis* (*B. subtilis*) effectively catalyzed luminol-H_2O_2 reaction to create excellent chemiluminescence (CL) signal because CotA-laccase exists on their surface. Based on these findings, a new CL biosensor via coupling to biological reaction system was presented for Glyp detection. The CL biosensor exhibited several advantages, such as eco-friendliness, low cost, high selectivity and sensitivity, and good practical application prospects for environmental pollution control.

1. Introduction

Glyp [N-(phosphonomethyl) glycine] is the most extensively used herbicide due to its low production cost, high effectiveness, non-selectivity, and broad-spectrum for killing a wide variety of

* Corresponding author. State Key Laboratory of Agricultural Microbiology, Huazhong Agricultural University, Wuhan, 430070, China.
** Corresponding author. State Key Laboratory of Agricultural Microbiology, Huazhong Agricultural University, Wuhan, 430070, China.
E-mail addresses: ruanlifang@mail.hzau.edu.cn (L. Ruan), yongganghu@mail.hzau.edu.cn (Y. Hu).
[1] Authors contributed equally to this work.

https://doi.org/10.1016/j.aca.2020.07.077
0003-2670/

plants by specifically inhibiting 5-enolpyruvylshikimate-3-phosphate synthase in the shikimate pathway. This inhibition blocks the synthesis of aromatic amino acids in plants, which eventually leads to plant death [1,2]. After foliar treatment, Glyp can be absorbed by leaves and then migrates toward other tissues, including roots, tubers, leaves, flowers, and seeds [3]. Glyp is widely distributed and accumulated in organs like leaves and seeds of Glyp-resistant crops (GRCs), hence it can be easily transferred to human and animal feed [4–6]. In addition to residues in farm products, partial Glyp moves to the soil from GRCs by root exudation. This movement ultimately leads to Glyp accumulation in soil and then migration from the ground to water over time. Glyp residues have been widely observed in soil, surface water, and underground water in the United States and other countries, where GRCs are commercially planted [7–9]. Recent studies have pointed out that Glyp residues in the environment and farm products pose not only ecological and agricultural risks to human beings and animals but also a serious public health concern [10].

The maximum residue level for Glyp in drinking water currently set by the World Health Organization is 0.90 mg L^{-1} [11]. Thus, detecting Glyp in the environment and farm products is urgently needed to avoid undesirable consequences. Among numerous analytical methods, liquid chromatography coupled with mass spectrometry (LC-MS/MS) [12], ion-exchange chromatography coupled to a pulsed amperometric detector [13], and ion chromatography [14] or gas chromatography coupled to a mass spectrometer [15] are widely employed for detection of Glyp. These methods offer sensitive and accurate detection results. However, they are often time-consuming, use complex procedures that require professional technical personnel, and involves Glyp derivatization to achieve the required limit of detection (LOD). Enzymes exhibit various features, including high catalytic efficiency, selectivity, and ease of operation under mild conditions of temperature and pH with appreciable reaction rates. The development of an enzyme-based biosensor is a promising alternative for Glyp measurement because it offers advantages, such as ease of operation, eco-friendliness, short detection time, low cost, and point-of-care monitoring. At present, few electrochemical biosensors were constructed for Glyp detection based on the inhibitory effect of Glyp on horseradish peroxidase (HRP) [16], atemoya peroxidase [17], and urease [18]. Nevertheless, their advantages are shadowed by complicated synthesis processes, complex enzyme electrode assembly, sophisticated measurement systems, and high material cost. Thus far, the use of specific enzymes for Glyp detection has not been reported yet. Developing specific enzymes for Glyp detection is essential and highly desirable for cost-effective estimation of Glyp with acceptable sensitivity and selectivity.

Glycine oxidase (GO) from *Bacillus* species is a flavoenzyme that consists of four homologous subunits; each subunit contains one molecule of noncovalently bound flavin adenine dinucleotide (FAD) [19,20]. This enzyme catalyzes the glycine oxidation in the biosynthesis of the thiamine thiazole ring, yielding the α-keto acids, ammonia/amine, and H_2O_2. Several GO such as BsuGO, BceGO, and BliGO from *B. subtilis*, *Bacillus cereus*, and *Bacillus licheniformis*, respectively, exhibit very low selectivity, affinity and poor kinetic efficiency for Glyp degradation through carbon–nitrogen (C–N) cleavage, yielding AMPA (aminomethylphosphonic acid), glyoxylate, and H_2O_2 in the presence of dissolved oxygen, although they prefer the glycine substrate [21,22]. The enzyme activity for the detection of Glyp can be effectively improved via genetic engineering technology. Recently, classic DNA shuffling and error-prone PCR approaches were combined to improve the substrate affinity and catalytic efficiency of these enzymes mentioned above. The resulted mutants exhibited higher oxidase activity on Glyp than that of the wild-type [23,24]. However, the obtained GO mutants retained their catalytic efficiency towards glycine. In addition, the initial motivation for developing Glyp-degrading enzymes was to develop new GRCs with high Glyp resistance. To the best of our knowledge, no reports can be found at present on the use of GO and its variants for Glyp detection.

Bacillus spores are a robust dormant structure formed during a remarkable phase in the life cycle of some bacteria. Spores can hold stability and long-term survival, even in hard conditions. Several kinds of spore-based whole-cell biosensors have been constructed using engineered spores [25–28]. Compared with other whole-cell biosensors, such as bacteria-based biosensors [29], spore-based whole-cell biosensors exhibit several advantages, such as recyclability, stability, easy operation, storage, and widespread application. Considering the presence of laccase (i.e., CotA protein) on the surfaces of *Bacillus* spores, we presented two whole-cell biosensors for antioxidant activity [30] and phenol assays [27] based on wild-type spores catalyzed under different color reactions. *Bacillus* spores showed a potential research value and application prospects in analytical determination.

Herein, the BceGO mutants were further evolved using protein engineering to extend the substrate selectivity and achieve high Glyp affinity. A high-activity and -selectivity variant B5R18 for Glyp instead of glycine was obtained for rapid Glyp degradation to yield AMPA, glyoxylate, and H_2O_2. Furthermore, a CL system was designed to detect H_2O_2 on the basis of *B. subtilis* spores catalyzed under the luminol-H_2O_2 reaction because of the existence of CotA-laccase on their surface (Scheme 1). A cascade reaction based on B5R18 coupled to the spores was developed for the detection of Glyp with high selectivity and sensitivity.

2. Experimental section

2.1. Construction of DNA shuffling mutant library

DNA shuffling was carried out to construct a mutant library with the methods described previously [31]. Briefly, 1.10 kb DNA fragment encoding each GO mutants were amplified with the plasmid pGEX-6P–B4S4, pGEX-6P–B4S6, pGEX-6P–B4S7, pGEX-6P–B4S9 and pGEX-6P–B4S11 as templates respectively, using 6P–1F and 6P-1R as universal primers (Table S1). Five PCR products were purified, mixed equally, and then fragmented by ultrasound treatment. The resulting fragments of 100–200 bp were used to reassemble into a full-length gene by primerless PCR reaction with following settings: 3 min at 95 °C, then 65 cycles (94 °C for 30 s, 40 °C for 30 s, 30 s + 1 s per cycle at 72 °C), followed by 10 min at 72 °C. Thereafter, the reassembled gene of accurate size was obtained by PCR with primeless reaction product (10-fold dilution with ultrapure water) as a template and oligonucleotide primers BceGO-F and BceGO-R((sequence shown in supplementary) under the reaction conditions: 94 °C for 3 min, 30 cycles (30 s at 94 °C, 90 s at 62 °C, 60 s at 72 °C), at last 72 °C for 10 min. The purified PCR product, digested by *BamH*I and *Xho*I, was ligated into the same enzymes digested expression vector pGEX-6P-1, and the recombinant plasmids were transformed into *E. coli* DH5α competent cells for further screening.

2.2. Screening of improved mutants activity for Glyp oxidation

To obtain variants of high oxidation activity towards Glyp, a method of enzyme-coupled colorimetric assay combined with bacteriophage-T7-induced cell lysis was employed for high-throughput selection of the mutant library. Transformants were cultivated in 96-deep-well plates containing 0.60 mL of LB medium comprising 0.10 mg mL^{-1} ampicillin overnight at 37 °C, and

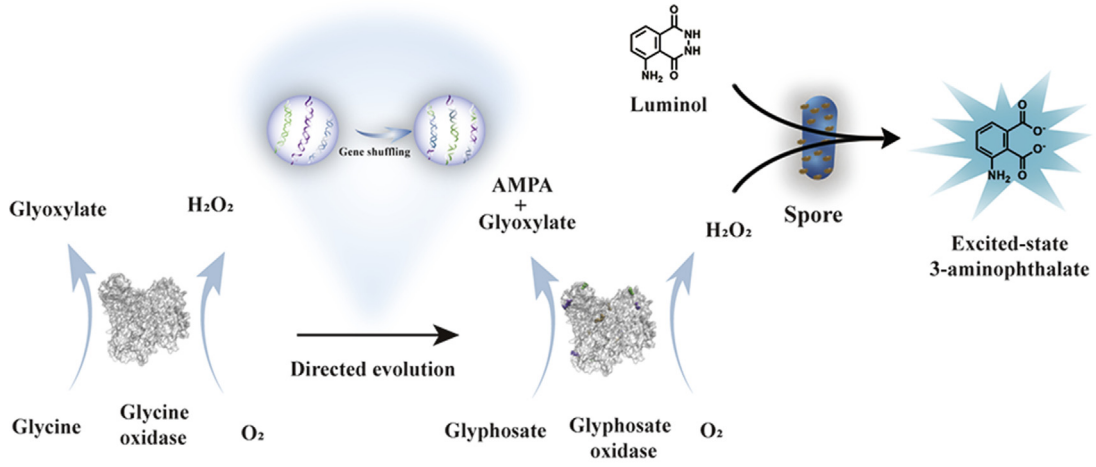

Scheme 1. Mechanism of engineered B5R18 coupled to spore-based CL system for Glyp detection.

duplication for each transformant had been grown on LB agar plate. Then, 0.10 mmol L^{-1} of IPTG and bacteriophage T7 were added into the 96-deep-well plate, followed by incubation at 28 °C with shaking for 6 h to synchronize the IPTG-induced enzyme expression and lysis of the recombinant *E.coli* cells. The activity of the lysate from each well was assayed by the enzyme-coupled colorimetric assay, as described in our earlier report [31].

2.3. Preparation of CotA of B.subtilis and cotA-knockout B.subtilis strain

CotA expression of *B.subtilis* was heterologously produced in *E.coli* Rosetta (DE3) strain by the use of the pET-28a plasmid. The cultivation of recombinant and CotA purification were performed according to previous work [32]. The knock-out of *cotA* gene was performed as a homologous double exchange in *B.subtilis* strain by use of the pDG780. The *cotA*-knockout process by our previously reported work [30].

2.4. Preparation of spores

B.subtilis spores were cultured by our previous method [32]. Briefly, *B. subtilis* was cultured in LB solid medium (added 0.25 mmol L^{-1} Cu^{2+}) at 37 °C for a week. The spores were scraped from solid medium and washed with ultrapure water for 5 times by centrifugation to remove the medium and cell debris, and then stored at 4 °C for next usage.

2.5. H_2O_2 detection using spore-based CL system

H_2O_2 was realized as follows: 10.00 μL of 2.00×10^{-4} mol L^{-1} luminol, and 10.00 μL of 2.00×10^{7} CFU mL^{-1} spore were added into 0.16 mL of CBS (pH 9.70). 20.00 μL of H_2O_2 was auto-injected and measured by an automatic sampler of Fluoroskan Ascent FL Multifunctional microplate reader (Thermo Fisher scientific, Waltham, MA, USA). Typical CL emission spectra were analyzed using by Shimadzu RF-5301PC fluorescence spectrophotometer (Tokyo, Japan).

2.6. Glyp detection using spore-luminol coupling with GlypO system

Glyp degradation by GlypO was conducted in a 0.10 mL reaction system containing 10.00 μL of 11.40 mg mL^{-1} GlypO, 10.00 μL of different concentration Glyp was added into 80.00 μL disodium pyrophosphate buffer (pH 7.00, 0.10 mol L^{-1}) at 25 °C for 1 h. 40.00 μL of the mixture was added into the follow system: 10.00 μL of 2.00×10^{-4} mol L^{-1} luminol, 10.00 μL of 2.00×10^{7} CFU mL^{-1} spore, and 0.14 mL of CBS (pH 9.70), and then the CL signal was measured with the luminescence analyzer.

3. Results and discussion

3.1. Engineered B5R18 with high activity and preference on Glyp

We previously utilized directed evolution to engineer BceGO substrate preference and activity, we obtained several mutants with higher oxidase activity on Glyp than wild-type BceGO [23,24]. Among the mutants, B4S7 is the best variant obtained from the second iteration of directed evolution. However, the degradation efficiency and selectivity are insufficient to meet the requirement for Glyp detection. Five BceGO variants, namely, B4S7, B4S4, B4S6, B4S9, and B4S11, were subjected to the third iteration of directed evolution by using their sequences as the starting sequence for constructing DNA shuffling mutant library. The libraries of the shuffled gene variants were screened by a high-throughput method to obtain new variants with high catalytic efficiency and selectivity toward Glyp detection.

Two mutants, namely, B5R18 and B5R26, which outperformed B4S7, were selected from 1.10×10^{4} transformants for further activity analysis. Their DNA sequences (Fig. S1) were measured, and the amino acid sequence of each variant was deduced by translating the corresponding DNA sequence (Fig. S2). The two mutants were then compared with B4S7, and their amino acid substitutions are shown in Table 1.

B5R18 and B5R26 were expressed in *E. coli* BL21 (DE3) and purified by affinity chromatography (Supplementary Information, Section 1.2). A single band (≈42.00 kDa) was observed in the SDS-PAGE images (Fig. 1A), suggesting high purity. The activities of B5R18 and B5R26 toward Glyp were evaluated by measuring H_2O_2

Table 1
Amino acid substitutions of B5R18 and B5R26 compared to that of B4S7.

Variant	Amino acid substitution
B5R18	D103Y, D121G, S122P, R238K, K367R, T368R
B5R26	S122P, H164R, Q346R, E357G, K367R, T368R

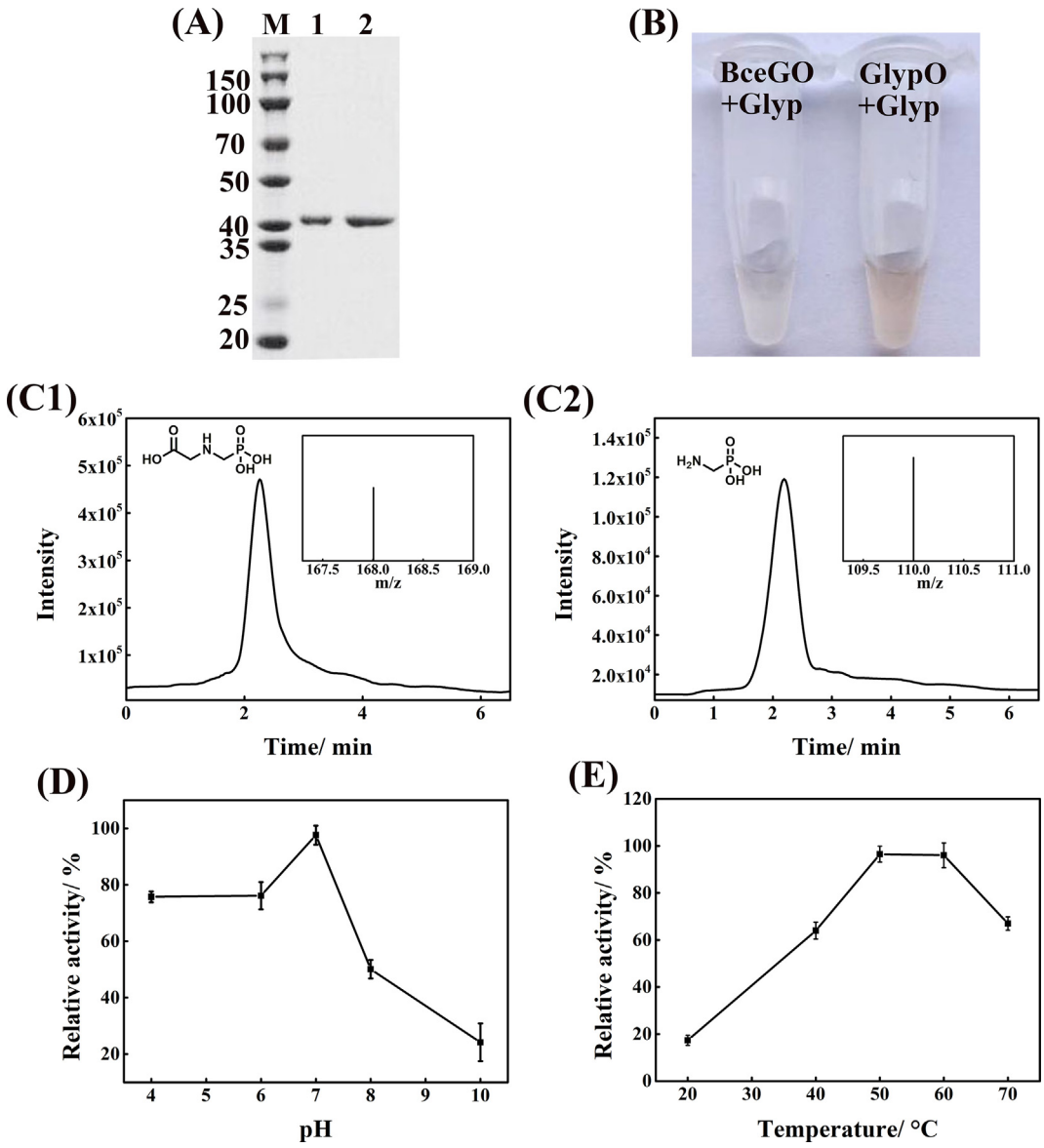

Fig. 1. (A) SDS-PAGE analysis of B5R18 and B5R26. Lane M, marker; Lane 1, B5R18; Lane 2, B5R26. (B) Glyp degradation by BceGO and GlypO, detected by the HRP/o-dianisidine spectrophotometric assay. Before (C1) and after (C2) Glyp degradation by GlypO, determined by UPLC-MS/MS. Insert: mass-to-charge ratio (m/z) of substrate (C1, Glyp) and product (C2, AMPA). The effect of pH (D) and temperature (E) on the relative activity of GlypO used for Glyp degradation. Condition: 5.00 mmol L^{-1} of Glyp, 0.032 mg L^{-1} of o-dianisidine dihydrochloride, 1.00 U mL^{-1} of HRP, a fixed amount of GlypO, at 25 °C (D), at pH 7.00 (E). These data represent means ± SE (n = 6).

at 25 °C through HRP/o-dianisidine spectrophotometric assay (Supplementary Information, Section 1.3). The catalysis reaction obeyed Michaelis–Menten theory (Fig. S3). Affinity (K_1, L $mmol^{-1}$), catalytic efficiency (K_2, L min^{-1} $mmol^{-1}$), affinity enhancement factor (K_3, was defined as the affinity ratio between Glyp and glycine), and specificity constant (K_4) of the enzymes for Glyp degradation were calculated (Supplementary Information, Section 1.3). As shown in Table 2, B5R18 showed a 1.96-fold decrease in K_m value (reached to 0.051 mmol L^{-1}) compared with the parent B4S7, suggesting a 2.31-fold increase in the affinity enhancement factor (K_3, reached 1.16 × 10^3) toward Glyp. A 2.70-fold increase in K_{cat} resulted in a 5.28-fold increase in the catalytic efficiency (K_2, from

Table 2
Comparison of the kinetics constants on Glyp and glycine determined for wild-type and variants of GO obtained by this work and other reports.

Enzyme	Glyp				Glycine				K_3	K_4
	K_{cat} (min^{-1})	K_m (mmol L^{-1})	K_1 (L $mmol^{-1}$)	K_2 (L min^{-1} $mmol^{-1}$)	K_{cat} (min^{-1})	K_m (mmol L^{-1})	K_1 (L $mmol^{-1}$)	K_2 (L min^{-1} $mmol^{-1}$)		
BceGO	5.72	84.79	0.012	0.067	8.17	1.04	0.96	7.86	0.012	0.0085
GAH [34]	63.00	0.50	2.00	126.00	90.00	105.00	0.0095	0.86	210.00	146.51
B4S7	3.62	0.10	10.00	36.20	2.18	50.34	0.020	0.043	503.40	841.86
B5R26	11.43	0.061	16.40	187.38	9.48	33.47	0.030	0.28	549.69	669.21
B5R18	9.74	0.051	19.61	190.98	6.18	59.02	0.017	0.10	1.16 × 10^3	1.91 × 10^3

36.20 min^{-1} mmol L^{-1} to 190.98 min^{-1} mmol L^{-1}) on Glyp. The specificity constant (K_4) reached 1.91 × 10^3, which was about 2.27-fold higher than that of B4S7 (841.86). The catalytic efficiency of B5R26 toward Glyp also increased 4.18-fold. However, the catalytic efficiency toward glycine increased 5.50-fold (0.28 versus 0.043 min^{-1} mmol L^{-1}), leading to 1.26-fold drop in the specificity constant (669.21 versus 841.86) and no significant change in the affinity enhancement factor (549.69 versus 503.40) toward Glyp. Thus, the specificity and affinity enhancement factors of B5R18 were 2.85- and 2.11-fold higher than those of B5R26, but their catalytic efficiencies toward Glyp were similar.

Table 2 reveals that the activity of B5R18 was superior to that of other enzymes. The catalytic efficiency, specificity constant, and affinity enhancement factor toward Glyp were 1.52-fold, 13.01-fold, and 5.51-fold higher than the mutant GAH (G51S/A54R/H244A) [33], respectively. Compared with the wild-type BceGO, B5R18 showed a 2.85 × 10^3-fold increase in the catalytic efficiency toward Glyp and a 78.60-fold decrease toward glycine, indicating 2.25 × 10^5-fold and 9.64 × 10^4-fold increase in the specificity constant and affinity enhancement factor toward Glyp, respectively. The evolved BceGO enzyme preferred substrate Glyp over glycine. Therefore, B5R18 was assigned as GlypO and chosen for subsequent experiments.

The protein band of GlypO was further analyzed by LC-MS/MS (Supplementary Information, Section 1.4). The molecular weight was 4.12 × 10^4 Da, which agreed with the theoretical value of BceGO. The coverage of the amino acid sequence reached 99.73% compared with the theoretical value (Fig. S4). These results demonstrated the successful cloning and expression of GlypO. The reaction of Glyp (10.00 mg L^{-1}) degradation catalyzed by GlypO in the presence of dissolved oxygen was further analyzed by UPLC-MS/MS and spectrophotometric assay (Supplementary Information, Section 1.5). The color change (Fig. 1B) demonstrated the production of H_2O_2. In comparison with the results in Fig. 1C 1, 99.00% Glyp was converted into AMPA within 3 h (Fig. 1C2), indicating the excellent Glyp degradation ability of GlypO.

The biochemical characterization of GlypO was investigated (Supplementary Information, Section 1.6). The effects including pH and temperature on the Glyp degradation by GlypO were investigated, respectively. The degradation efficiency was increased as the pH increased from 4.00 to 7.00 (Fig. 1D). And then the degradation efficiency reached the maximum value when the pH in the reaction system was 7.00. The activity drops substantially above pH 7.00. GlypO exhibited high relative activity in the range of 50–60 °C, but significantly lost the catalytic activity when the temperature increased higher than 60 °C (Fig. 1E). These results indicated that GlypO exhibited high activity at pH 7.00 during 50–60 °C. The effects of temperature and pH on the stability of GlypO were also investigated, respectively. First, GlypO was pretreated by incubating it at different temperature (10–70 °C) for 1 h at pH 8.50. GlypO could retain high activity in the temperature range of 10–50 °C and significantly lost the activity when the temperature increased higher than 50 °C (Fig. S5A), demonstrating that GlypO has more resistant on higher temperature. Second, GlypO was incubated in different pH solutions (4.00–11.00) for 6 h at 4 °C. Results shown in Fig. S5B indicate that GlypO could retain 100.00% activity at 7.00, and the relative activity lost at other investigated pH conditions. That is, GlypO has good stability at pH 7.00.

The effects of ions (e.g., KCl, KBr, NaCl, $MgSO_4$, NH_4Cl, K_2SO_4, $CaCl_2$, and $MgCl_2$) on the relative activity of the enzyme were studied by measuring enzyme activity in the presence of each ion at a final concentration of 10.00 mmol L^{-1} (Fig. S5C). KCl, KBr, NaCl, K_2SO_4, and $CaCl_2$ did not affect the GlypO activity. Over 20.00% of the relative activity decreased in the presence of $MgSO_4$ and $MgCl_2$, possibly because the stability of FAD was inhibited by Mg^{2+} [34]. The activity of GlypO slightly decreased in the presence of NH_4^+ possibly because NH_4^+ could affect the pH of the incubated system.

3.2. Spore-luminol CL system for H_2O_2 detection

Developing a GlypO-based biosensor for specific detection of Glyp via H_2O_2 measurement has good prospects owing to its outstanding selectivity, affinity, and activity toward Glyp degradation to yield H_2O_2. For the first time, we found that the spores of *B. subtilis* could catalyze the luminol-H_2O_2 reaction to produce a high CL signal. In this regard, we can develop a new CL method for Glyp detection.

The spore-luminol-H_2O_2 CL reaction was investigated in detail. As shown in Fig. 2A, the maximum emission peak was centered at 425.00 nm, indicating that the luminophor was the excited state 3-aminophthalate anions (3-APA*). We believe that the ability of spores to catalyze luminol-H_2O_2 reaction is due to the presence of CotA on their surface because commercial laccase could be used to catalyze luminol CL in the presence of H_2O_2 [35]. To verify this hypothesis, we expressed the recombinant CotA-laccase from *B. subtilis* in the *E. coli* system. SDS-PAGE and Western blot analyses were used for protein verification, and the results suggested that a specific band appeared at the site of 65.00 kDa molecular weight, indicating successful cloning and expression of CotA-laccase (Fig. 2B1 and 2B2). As a control, the *cotA* gene was knocked out from the *B. subtilis* genome by homologous double exchange method involving exchange with the *kanamycin* gene. The *kanamycin* gene fragment (794 bp) was obtained, and the *cotA* gene fragment (500 bp) disappeared through the genome PCR of the *cotA*-knockout mutant strain. The findings demonstrated that the *cotA* gene was replaced by the *kanamycin* gene (Fig. 2C).

Spores, the *cotA* knock-out strain spores (Mt-spores), laccase, and CotA were mixed with the luminol-H_2O_2 solution. As shown in Fig. 2D, the spores, laccase, and CotA catalyzed the luminol-H_2O_2 reaction to produce a high CL signal. However, no CL signal was observed in the Mt-spore-luminol-H_2O_2 system. These results confirmed that CotA-laccase on the spore surface is the key to catalyz the luminol CL reaction in the presence of H_2O_2. A spore-based whole-cell CL system was then established for H_2O_2 detection. Under the optimal conditions (Supplementary Information, Section 2.1; and Fig. S6, pH 9.70, 0.010 mmol L^{-1} of luminol, 1.00 × 10^6 CFU mL^{-1} of spore), the CL intensity increased with increasing H_2O_2 concentration (Fig. 2E). A good linear proportion was observed between within 0.050–20.00 μmol L^{-1} with the following equation:

$$Y = 800.07X + 47.54 \ (R^2 = 0.996) \quad (7)$$

where Y is the CL intensity, and X is the H_2O_2 concentration (μmol L^{-1}). The LOD of

H_2O_2 was 0.050 μmol L^{-1} (S/N = 3), which is higher than those of most relevant literature reports for H_2O_2 detection and only comparable to those of Co-MOF-based CL method and Hemin/RGO-CMF-based electrochemistry method (Table 3). There are several advantages to the use of spore, such as no complex synthesis procedure, low cost, stability, and eco-friendliness compared with nanomaterials. As shown in Fig. 2F, the catalytic activity of spores for luminol-H_2O_2 remained stable for 42 d when stored in distilled water at room temperature. The findings also revealed the excellent storage stability of the spores. The higher storage stability of spores than that of commercial enzymes and purified protein, reduced not only the cost but also maintained stable detection.

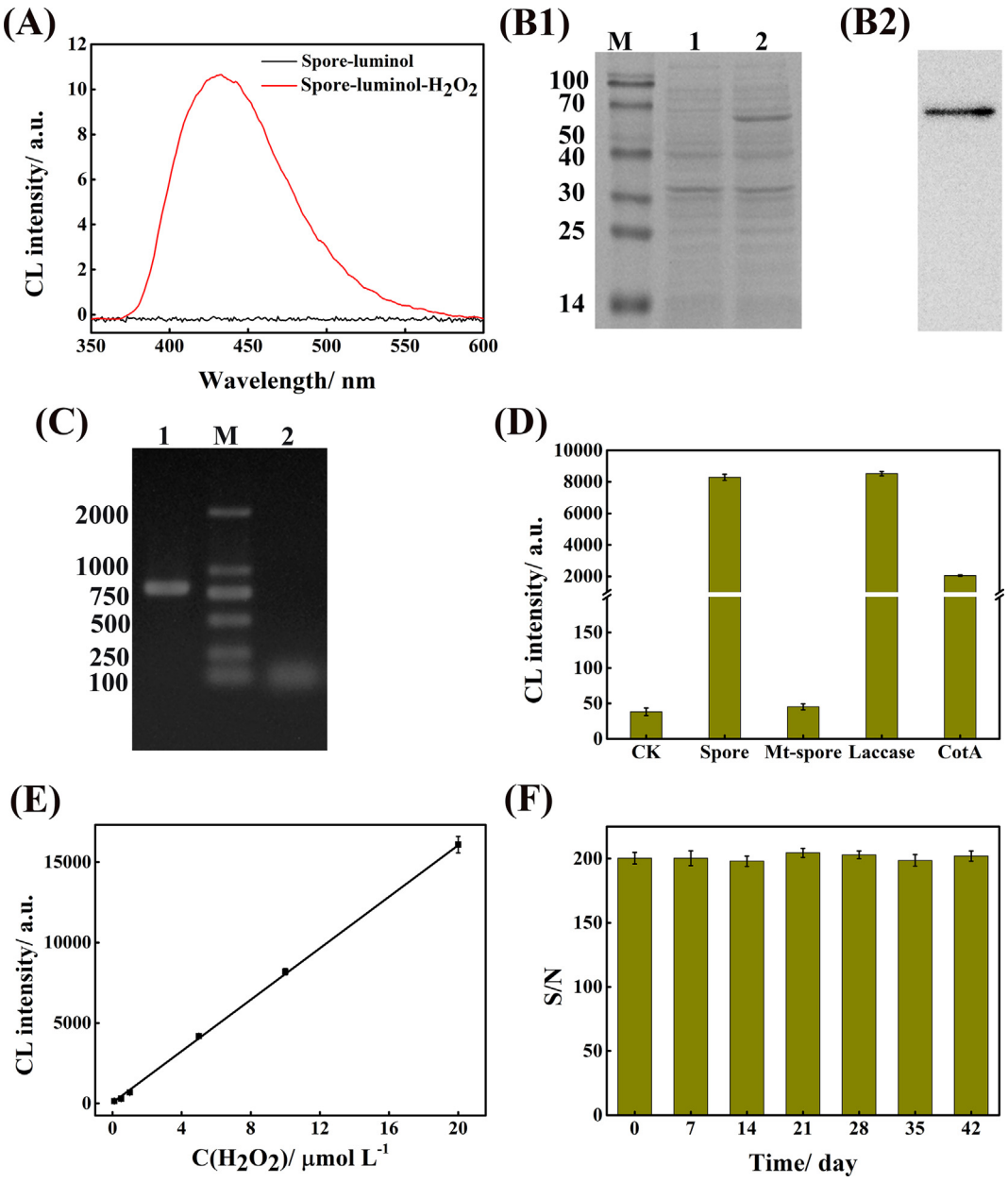

Fig. 2. (A) CL spectra for the spore-luminol and spore-luminol-H_2O_2 CL reactions. (B1) SDS-PAGE results of CotA protein expressed by *E.coli.* M, maker; the cell extracts before (2) after (3) induction by IPTG. (B2) Western blot result of obtained CotA protein. (C) Agarose gel electrophoresis of genome PCR products of *cotA*-knockout mutant strain amplified using primers of the *kanamycin* gene and *cotA* gene. Lane M, marker; Lane 1, *kanamycin* gene; Lane 2, *cotA* gene. (D) The CL intensity of luminol-H_2O_2 catalyzed using spore, Mt-spore, laccase, and CotA, respectively. CK: No catalyst was added. (E) Spore-based CL system used for H_2O_2 determination. (F) The CL stability of spores in the H_2O_2 detection within 42 days. Conditions: pH 9.70, 0.010 mmol L^{-1} luminol, 1.00 × 10^6 CFU mL^{-1} spore, and 10.00 μmol L^{-1} H_2O_2. These data represent means ± SE (n = 6).

Table 3
Comparison of H_2O_2 detection by spore-based CL system and other methods.

Materials	Detection methods	Linear range (μmol L^{-1})	LOD (μmol L^{-1})	Refs
Hemin@HKUST-1	CL	7.5–750	7.5	[36]
Co-MOF	CL	0.04–8	0.01	[37]
Gold nanocluster	Fluorescent	1–100	0.8	[38]
2D Cu-MOF nanosheet	Fluorescent	0.32–60	0.32	[39]
Hemin/RGO-CMF	Electrochemistry	0.06–540.6	0.016	[40]
MNP@Au-PB	Electrochemistry	4–2.2 × 10^4	1.1	[41]
Cu-hemin MOFs	Colorimetry	1–1 × 10^3	0.42	[42]
Hemin@MIL-101(Al)–NH_2	Colorimetry	5–200	2	[43]
Spores	CL	0.05–20	0.050	This work

3.3. Spore-luminol coupling with GlypO CL system for Glyp detection

After full investigation, the engineered GlypO was coupled to the spore-luminol CL system for Glyp detection, which is proportional to the production of H_2O_2. Two steps were involved in the spore-based CL biosensor for Glyp. First, the formation of H_2O_2 produced due to the degradation of Glyp at pH 7.00. Second, the production containing H_2O_2 was then added into a spore-luminol mixture solution (pH 9.70). The concentration of H_2O_2 was measured by the CL reaction of spore-luminol- H_2O_2.

Glyp and its degradation products, including AMPA, glyoxylate, and H_2O_2, were mixed with the spore-luminol solution. Only spore-luminol-H_2O_2 created a high CL signal (Fig. 3A). These results demonstrated that the spore-based CL sensor could act as a highly selective and sensitive method for Glyp detection by measuring H_2O_2 produced by the GlypO catalysis reaction. The CL intensity was linearly proportional to the Glyp concentration within 0.090–75.00 mg L^{-1} (Fig. 3B), as calculated using the following equation:

$$Y = 170.71X + 120.00 \ (R^2 = 0.997) \quad (8)$$

where Y is the CL intensity, and X is the Glyp concentration (mg L^{-1}). The LOD of Glyp was 0.090 mg L^{-1} (S/N = 3), which was sufficient to meet the demands for drinking water (0.90 mg L^{-1}) and comparable to that of relevant literature reports (Table 4). The proposed CL method exhibited several advantages, including rapidity, high selectivity and sensitivity, relativity simple equipment, easy operation, and eco-friendliness.

The effects of adding interfering substances (glycine, glufosinate ammonium, AMPA, and PO_4^{3-}) with the same concentration for 0.059 mmol L^{-1} Glyp measure was investigated (Fig. 3C). The CL intensity of glycine, glufosinate ammonium, AMPA, and PO_4^{3-} was only 4.05%, 3.27%, 1.47%, and 2.05% of Glyp under the same concentration. Besides, the most abundant dissolved amino acid including glycine in natural waters range from 2.30 to 17.70 μg L^{-1} [48], and in drinking water range from 0.33 to 1.05 μg L^{-1} [49], which is 250.00 and 4.21 × 10^3-fold less than the one we tested (i.e., 0.059 mmol L^{-1}), respectively. The glycine might be therefore an ignorable interference factor for Glyp detection in real samples. Thus, the developed biosensor system has good selectivity and prospective for Glyp detection in natural and drinking water samples.

A recovery experiment in real samples was performed using the standard addition method. A total of 5.00 mg L^{-1} Glyp was added into deionized, tap, and lake water samples, which were then analyzed with a spore-based CL sensor (Table S1). The Glyp detection system displayed excellent performance with 102.00%–105.20% recovery, demonstrating its good accuracy and potential practical applications in natural water environments.

4. Conclusion

In this work, a GlypO preferring substrate Glyp over glycine, was obtained via directed evolution from BceGO. The catalytic efficiency, specificity constant, and affinity enhancement factor toward Glyp were increased by 2.85 × 10^3-fold; 2.25 × 10^5-fold; and 9.64 × 10^4-fold, respectively. Moreover, a spore-based CL whole-cell system for H_2O_2 detection was investigated in detail. Given that GlypO can selectively catalyze Glyp degradation to yield H_2O_2, a new CL biosensor for Glyp detection was then developed by coupling the

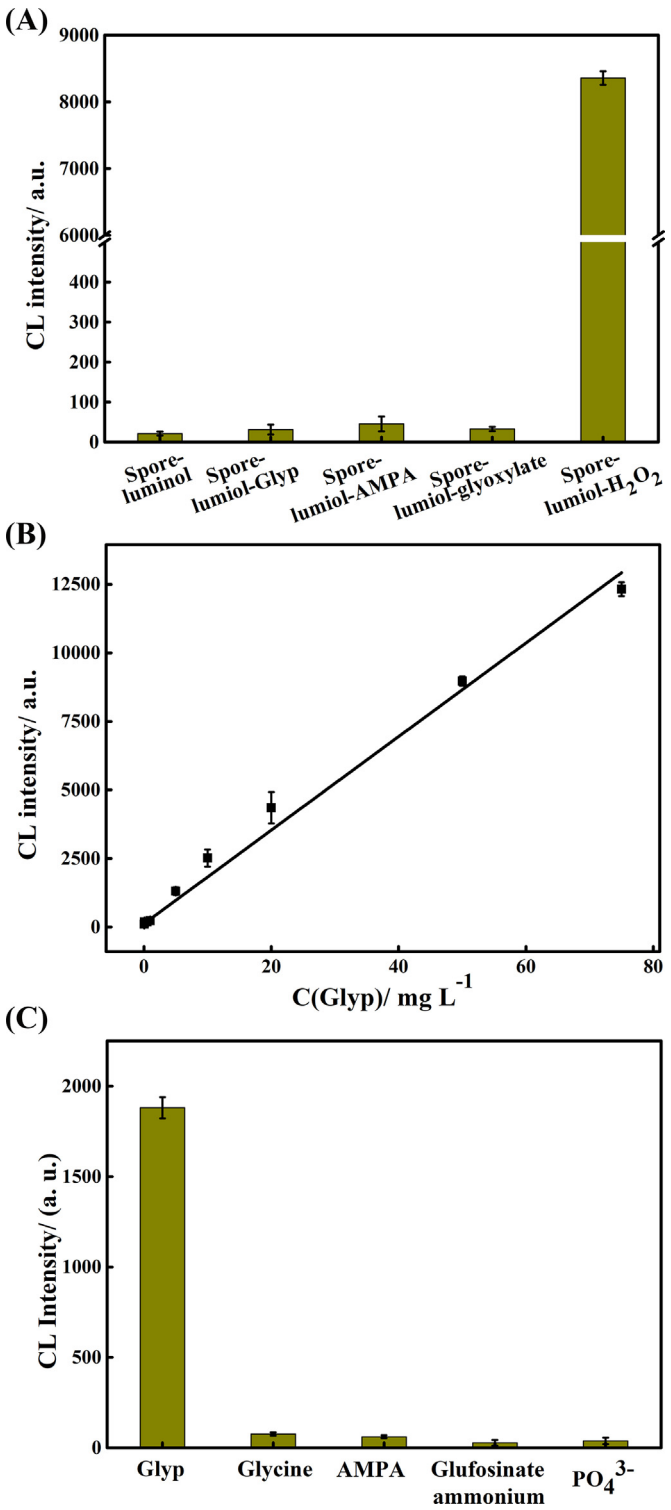

Fig. 3. (A) The CL reaction of spore-luminol in the presence of Glyp, AMPA, glyoxylate, and H_2O_2. Conditions: pH 9.70, 0.010 mmol L^{-1} luminol, and 1.00 × 10^6 CFU mL^{-1} spore in the presence of 0.030 mmol L^{-1} Glyp, glyoxylate, and AMPA, 10.00 μmol L^{-1} H_2O_2, respectively. (B) Spore-based CL system used for Glyp determination. Conditions: pH 9.70, 0.010 mmol L^{-1} luminol and 1.00 × 10^6 CFU mL^{-1} spore, 1.14 mg mL^{-1} GlypO, 0.090–75.00 mg L^{-1} Glyp. (C) The selectivity for Glyp detection with the proposed CL assay. Conditions: pH 9.70, 0.010 mmol L^{-1} of luminol and 1.00 × 10^6 CFU mL^{-1} spore, 1.14 mg mL^{-1} GlypO, 0.059 mmol L^{-1} of Glyp, glycine, AMPA, glufosinate ammonium, and PO_4^{3-}. These data represent means ± SE (n = 3).

Table 4
Comparison of Glyp detection by proposed system and other methods.

Methods	Detection targets	Linear range (mg L^{-1})	LOD (mg L^{-1})	Refs
Fe_3O_4@SiO_2@UiO-67	Organophosphorus	0.1–40	0.093	[44]
Fluorescent carbon dots	Glyp	0.338–4.056	0.101	[18]
Cu^{2+}/TMB/H_2O_2	Glyp	0.338–33.8	0.169	[45]
Oligopeptide functionalized surface plasmon resonance	Glyp	–	0.098	[46]
Integrated pulsed amperometric/anion-exchange chromatography	Glyp	0.01–5	0.05	[13]
Capillary electrophoresis/electrochemiluminescence	Glyp	0.169–16.9	0.06	[47]
Spore-luminol-GlypO CL system	Glyp	0.09–75	0.09	This work

engineered enzyme to the spore-based system. The CL intensity was linearly proportional to the Glyp concentration within 0.09–75.00 mg L^{-1}. The LOD of Glyp was 0.090 mg L^{-1} (S/N = 3), which met the demands for drinking water. The proposed biosensor has several advantages, including high selectivity and sensitivity, low cost, stability, and eco-friendliness, and thus has potential practical applications for environmental pollution control.

CRediT authorship contribution statement

Yuqing Qin: Methodology, Software, Validation, Formal analysis, Investigation, Writing - original draft, Visualization. **Gaobing Wu:** Conceptualization, Resources, Writing - review & editing, Funding acquisition, Investigation. **Yiming Guo:** Methodology, Software, Writing - original draft, Investigation. **Da Ke:** Investigation, Formal analysis. **Jiakang Yin:** Software. **Donglin Wang:** Investigation, Methodology. **Xuezhu Fan:** Investigation, Methodology. **Ziduo Liu:** Investigation. **Lifang Ruan:** Conceptualization, Supervision, Writing - review & editing. **Yonggang Hu:** Conceptualization, Resources, Writing - review & editing, Supervision, Project administration, Funding acquisition.

Declaration of competing interest

The authors declare that they have no known competing financial interests or personal relationships that could have appeared to influence the work reported in this paper.

Acknowledgements

This study was supported by grants from the National Transgenic Major Project of China (no. 2018ZX0800906B), the National Natural Science Foundation of China (no. 21675057, 31970123, 31971383), and the Fundamental Research Funds for the Central Universities (no. 2662018JC015, 2662018PY054).

Appendix A. Supplementary data

Supplementary data to this article can be found online at https://doi.org/10.1016/j.aca.2020.07.077.

References

[1] S. Eker, L. Ozturk, A. Yazici, B. Erenoglu, V. Romheld, I. Cakmak, Foliar-applied glyphosate substantially reduced uptake and transport of iron and manganese in sunflower (Helianthus annuus L.) plants, J. Agric. Food Chem. 54 (2006) 10019–10025.
[2] T. Zhan, K. Zhang, Y.Y. Chen, Y.J. Lin, G.B. Wu, L.L. Zhang, P. Yao, Z.Z. Shao, Z.D. Liu, Improving glyphosate oxidation activity of glycine oxidase from *Bacillus cereus* by directed evolution, PloS One 8 (2013) 10.
[3] M.P. Gomes, E. Smedbol, A. Chalifour, L. Henault-Ethier, M. Labrecque, L. Lepage, M. Lucotte, P. Juneau, Alteration of plant physiology by glyphosate and its by-product aminomethylphosphonic acid: an overview, J. Exp. Bot. 65 (2014) 4691–4703.
[4] J. Xu, S. Smith, G. Smith, W. Wang, Y. Li, Glyphosate contamination in grains and foods: an overview, Food Contr. 106 (2019) 106710.
[5] H. Fu, S. Qiu, X. Yao, F. Gao, P. Tan, T. Teng, B. Shi, Toxicity of glyphosate in feed for weanling piglets and the mechanism of glyphosate detoxification by the liver nuclear receptor CAR/PXR pathway, J. Hazard Mater. 387 (2020) 121707.
[6] L. Trasande, S.I. Aldana, H. Trachtman, K. Kannan, D. Morrison, D.A. Christakis, K. Whitlock, M.J. Messito, R.S. Gross, R. Karthikraj, S. Sathyanarayana, Glyphosate exposures and kidney injury biomarkers in infants and young children, Environ. Pollut. 256 (2020) 113334.
[7] S. Gunarathna, B. Gunawardana, M. Jayaweera, J. Manatunge, K. Zoysa, Glyphosate and AMPA of agricultural soil, surface water, groundwater and sediments in areas prevalent with chronic kidney disease of unknown etiology, Sri Lanka, J. Environ. Sci. Health Part B–Pestic. Contam. Agric. Wastes 53 (2018) 729–737.
[8] V. Silva, L. Montanarella, A. Jones, O. Fernández-Ugalde, H.G.J. Mol, C.J. Ritsema, V. Geissen, Distribution of glyphosate and aminomethylphosphonic acid (AMPA) in agricultural topsoils of the European Union, Sci. Total Environ. 621 (2018) 1352–1359.
[9] A.H.C. Van Bruggen, M.M. He, K. Shin, V. Mai, K.C. Jeong, M.R. Finckh, J.G. Morris, Environmental and health effects of the herbicide glyphosate, Sci. Total Environ. 616–617 (2018) 255–268.
[10] A.L. Valle, F.C.C. Mello, R.P. Alves-Balvedi, L.P. Rodrigues, L.R. Goulart, Glyphosate detection: methods, needs and challenges, Environ. Chem. Lett. 17 (2019) 291–317.
[11] L.K.S. De Almeida, S. Chigome, N. Torto, C.L. Frost, B.I. Pletschke, A novel colorimetric sensor strip for the detection of glyphosate in water, Sensor. Actuator. B Chem. 206 (2015) 357–363.
[12] R. Gotti, J. Fiori, S. Bosi, G. Dinelli, Field-amplified sample injection and sweeping micellar electrokinetic chromatography in analysis of glyphosate and aminomethylphosphonic acid in wheat, J. Chromatogr. A 1601 (2019) 357–364.
[13] K. Sato, J.-Y. Jin, T. Takeuchi, T. Miwa, K. Suenami, Y. Takekoshi, S. Kanno, Integrated pulsed amperometric detection of glufosinate, bialaphos and glyphosate at gold electrodes in anion-exchange chromatography, J. Chromatogr. A 919 (2001) 313–320.
[14] J. You, J.A. Koropchak, Condensation nucleation light scattering detection with ion chromatography for direct determination of glyphosate and its metabolite in water, J. Chromatogr. A 989 (2003) 231–238.
[15] M.P.G. de Llasera, L. Gómez-Almaraz, L.E. Vera-Avila, A. Peña-Alvarez, Matrix solid-phase dispersion extraction and determination by high-performance liquid chromatography with fluorescence detection of residues of glyphosate and aminomethylphosphonic acid in tomato fruit, J. Chromatogr. A 1093 (2005) 139–146.
[16] E.A. Songa, T. Waryo, N. Jahed, P.G.L. Baker, B.V. Kgarebe, E.I. Iwuoha, Electrochemical nanobiosensor for glyphosate herbicide and its metabolite, Electroanalysis 21 (2009) 671–674.
[17] G.C. Oliveira, S.K. Moccelini, M. Castilho, A.J. Terezo, J. Possavatz, M.R.L. Magalhães, E.F.G.C. Dores, Biosensor based on atemoya peroxidase immobilised on modified nanoclay for glyphosate biomonitoring, Talanta 98 (2012) 130–136.
[18] C. Vaghela, M. Kulkarni, S. Haram, R. Aiyer, M. Karve, A novel inhibition based biosensor using urease nanoconjugate entrapped biocomposite membrane for potentiometric glyphosate detection, Int. J. Biol. Macromol. 108 (2018) 32–40.
[19] V. Job, G.L. Marcone, M.S. Pilone, L. Pollegioni, Glycine oxidase from *Bacillus subtilis*- Characterization of a new flavoprotein, J. Biol. Chem. 277 (2002) 6985–6993.
[20] V. Job, G. Molla, M.S. Pilone, L. Pollegioni, Overexpression of a recombinant wild-type and His-tagged *Bacillus subtilis* glycine oxidase in *Escherichia coli*, Eur. J. Biochem. 269 (2002) 1456–1463.
[21] M. Pedotti, E. Rosini, G. Molla, T. Moschetti, C. Savino, B. Vallone, L. Pollegioni, Glyphosate resistance by engineering the flavoenzyme glycine oxidase, J. Biol. Chem. 284 (2009) 36415–36423.
[22] L. Pollegioni, G. Molla, New biotech applications from evolved D-amino acid oxidases, Trends Biotechnol. 29 (2011) 276–283.
[23] P. Yao, Y. Lin, G. Wu, Y. Lu, T. Zhan, A. Kumar, L. Zhang, Z. Liu, Improvement of glycine oxidase by DNA shuffling, and site-saturation mutagenesis of F247 residue, Int. J. Biol. Macromol. 79 (2015) 965–970.
[24] G.B. Wu, T. Zhan, Y.M. Guo, A. Kumar, Z.D. Liu, Asn336 is involved in the substrate affinity of glycine oxidase from *Bacillus cereus*, Electron. J. Biotechnol. 22 (2016) 26–30.
[25] R. Fei, T. Zhang, Y. Huang, Y. Hu, Highly selective enrichment of phosphorylated proteins by using Spore@Fe^{3+} microspheres, Anal. Chim. Acta 986 (2017) 161–170.

[26] R.H. Fei, C. Tan, Y. Huang, H.C. Chen, A.Z. Guo, H.L. Wang, Y.G. Hu, Self-assembled Ti^{4+}@Biospore microspheres for sensitive DNA analysis, ACS Appl. Mater. Interfaces 9 (2017) 34696–34705.
[27] Z. Zeng, L. Tian, Z. Li, L. Jia, X. Zhang, M. Xia, Y. Hu, Whole-cell method for phenol detection based on the color reaction of phenol with 4-aminoantipyrine catalyzed by CotA laccase on endospore surfaces, Biosens. Bioelectron. 69 (2015) 162–166.
[28] Z.M. Zeng, Y. Zhong, H.C. Yang, R.H. Fei, R. Zhou, R. Luque, Y.G. Hu, Naturally nano: synthesis of versatile bio-inpired monodisperse microspheres from *Bacillus* spores and their applications, Green Chem. 18 (2016) 186–196.
[29] A. Lopreside, X. Wan, E. Michelini, A. Roda, B. Wang, Comprehensive profiling of diverse genetic reporters with application to whole-cell and cell-free biosensors, Anal. Chem. 91 (2019) 15284–15292.
[30] L.N. Jia, R.H. Fei, X.Y. Zhang, H.X. Tang, Y.G. Hu, Sustainable endospore-based microreactor system for antioxidant capacity assay, Anal. Chem. 86 (2014) 11578–11585.
[31] W.P. Stemmer, DNA shuffling by random fragmentation and reassembly: in vitro recombination for molecular evolution, Proc. Natl. Acad. Sci. U. S. A. 91 (1994) 10747–10751.
[32] Y. Qin, F. Peng, Y. Hu, Rapid catalytic oxidation of As(III) to As(V) using a *Bacillus* spore–2,2,6,6-tetramethylpiperidine-1-oxyl system, Green Chem. 21 (2019) 2286–2294.
[33] M. Pedotti, E. Rosini, G. Molla, T. Moschetti, C. Savino, B. Vallone, L. Pollegioni, Glyphosate resistance by engineering the flavoenzyme glycine oxidase, J. Biol. Chem. 284 (2009) 36415–36423.
[34] T. Hagihara, T. Fujio, K. Aisaka, Cloning of FAD synthetase gene from corynebacterium ammoniagenes and its application to FAD and FMN production, Appl. Microbiol. Biotechnol. 42 (1995) 724–729.
[35] Y. Zhag, C. Tan, R.H. Fei, X.X. Liu, Y. Zhou, J. Chen, H.C. Chen, R. Zhou, Y.G. Hu, Sensitive chemiluminescence immunoassay for *E. coli* O157:H7 detection with signal dual-amplification using glucose oxidase and laccase, Anal. Chem. 86 (2014) 1115–1122.
[36] F.Q. Luo, Y.L. Lin, L.Y. Zheng, X.M. Lin, Y.W. Chi, Encapsulation of hemin in Metal Organic Frameworks for catalyzing the chemiluminescence reaction of the H_2O_2-luminol system and detecting glucose in the neutral condition, ACS Appl. Mater. Interfaces 7 (2015) 11322–11329.
[37] D. Li, S. Zhang, X. Feng, H. Yang, F. Nie, W. Zhang, A novel peroxidase mimetic Co-MOF enhanced luminol chemiluminescence and its application in glucose sensing, Sensor. Actuator. B Chem. 296 (2019) 126631.
[38] H.-C. Chang, J.-a.A. Ho, Gold nanocluster-assisted fluorescent detection for hydrogen peroxide and cholesterol based on the inner filter effect of gold nanoparticles, Anal. Chem. 87 (2015) 10362–10367.
[39] M.Y. Shi, M. Xu, Z.Y. Gu, Copper-based two-dimensional Metal-Organic Framework nanosheets as horseradish peroxidase mimics for glucose fluorescence sensing, Anal. Chim. Acta 1079 (2019) 164–170.
[40] S. Wang, Y. Zhao, M. Wang, H. Li, M. Saqib, C. Ge, X. Zhang, Y. Jin, Enhancing luminol electrochemiluminescence by combined use of cobalt-based metal organic frameworks and silver nanoparticles and its application in ultrasensitive detection of cardiac troponin I, Anal. Chem. 91 (2019) 3048–3054.
[41] Y. Li, J. Liu, Y. Fu, Q. Xie, Y. Li, Correction to: magnetic-core@dual-functional-shell nanocomposites with peroxidase mimicking properties for use in colorimetric and electrochemical sensing of hydrogen peroxide, Microchim. Acta 186 (2019) 456.
[42] F. Liu, J. He, M. Zeng, J. Hao, Q. Guo, Y. Song, L. Wang, Cu–hemin Metal-Organic Frameworks with peroxidase-like activity as peroxidase mimics for colorimetric sensing of glucose, J. Nanoparticle Res. 18 (2016).
[43] F.X. Qin, S.Y. Jia, F.F. Wang, S.H. Wu, J. Song, Y. Liu, Hemin@metal-organic framework with peroxidase-like activity and its application to glucose detection, Catal. Sci. Technol. 3 (2013) 2761–2768.
[44] Q.F. Yang, J. Wang, X.Y. Chen, W.X. Yang, H.N. Pei, N. Hu, Z.H. Li, Y.R. Suo, T. Li, J.L. Wang, The simultaneous detection and removal of organophosphorus pesticides by a novel Zr-MOF based smart adsorbent, J. Mater. Chem. A 6 (2018) 2184–2192.
[45] Y. Chang, Z. Zhang, J. Hao, W. Yang, J. Tang, A simple label free colorimetric method for glyphosate detection based on the inhibition of peroxidase-like activity of Cu(II), Sensor. Actuator. B Chem. 228 (2016) 410–415.
[46] X. Ding, K.-L. Yang, Development of an oligopeptide functionalized surface plasmon resonance biosensor for online detection of glyphosate, Anal. Chem. 85 (2013) 5727–5733.
[47] H.Y. Chiu, Z.Y. Lin, H.L. Tu, C.W. Whang, Analysis of glyphosate and aminomethylphosphonic acid by capillary electrophoresis with electrochemiluminescence detection, J. Chromatogr. A 1177 (2008) 195–198.
[48] J.H. Lee, C. Na, R.L. Ramirez, T.M. Olson, Cyanogen chloride precursor analysis in chlorinated river water, Environ. Sci. Technol. 40 (2006) 1478–1484.
[49] S. Brosillon, M. Lemasle, E. Renault, D. Tozza, V. Heim, A. Laplanche, Analysis and occurrence of odorous disinfection by-products from chlorination of amino acids in three different drinking water treatment plants and corresponding distribution networks, Chemosphere 77 (2009) 1035–1042.